Journal of the Serbian Chemical Society
JSCS-info@shd.org.rs • www.shd.org.rs/JSCS
J. Serb. Chem. Soc. *84* (8) 801–817 (2019)
JSCS–5226
UDC 544.354–128.2:543.426.1:537.5:544.2.004.12
Original scientific paper

SCCS$^-$ radical: Renner–Teller effect and spin–orbit coupling in the X $^2\Pi_u$ electronic state

STANKA V. JEROSIMIĆ*, MARKO LJ. MITIĆ and MILAN Z. MILOVANOVIĆ

Faculty of Physical Chemistry, University of Belgrade, Studentski trg 12–16, PAC 105305, 11158 Belgrade, Serbia

(Received 1 April, accepted 6 May 2019)

Abstract: SCCS$^-$ was detected by laser-induced fluorescence spectroscopy in 2003 (M. Nakajima, Y. Yoneda, Y. Sumiyoshi, T. Nagata, Y. Endo, *J. Chem. Phys.* **119** (2003) 7805) and its spectrum was analyzed and the results presented together with *ab initio* calculations data. Symmetrical stretching vibrations were assigned in both the ground *X* $^2\Pi_u$ and the first excited *A* $^2\Pi_g$ electronic states, but no data about spin–orbit splitting and bending vibrational modes were given. In the present work, the vibronic levels in the ground electronic state of SCCS$^-$ were calculated by means of a model developed by Perić and coworkers for the treatment of the Renner–Teller effect in any-atomic linear species in its variational form (M. Mitić, R. Ranković, M. Milovanović, S. Jerosimić, M. Perić, *Chem. Phys.* **464** (2016) 55) using the *ab initio* multi-reference configuration interaction calculations for obtaining potential energy curves in the Born–Oppenheimer approximation. Additionally, the spin–orbit splitting in the ground state was investigated taking into account the interaction with the first excited state, and the energies obtained from combined treatment of vibronic and spin–orbit interactions in the ground state are reported. Finally, based on the present results, several assignments of unidentified bands reported by Nakajima *et al.* are proposed.

Keywords: vibronic levels; four-atomic molecules; $^2\Pi_u$ electronic state; MRCI-F12 calculations.

INTRODUCTION

Not many anions can have valence excited electronic states below the energy threshold for electron detachment. One such species is the SCCS$^-$ radical, which was obtained in a discharged supersonic jet of carbon disulphide, and observed by laser-induced fluorescence (LIF) spectroscopy.[1,2] This species was previously detected by mass spectrometry when $(CS_2)_n^-$ cluster was investigated by photodestruction spectroscopy.[3] From the spectrum obtained by the excitation scan

* Corresponding author. E-mail: stanka@ffh.bg.ac.rs
https://doi.org/10.2298/JSC190401033J

variant of LIF and fluorescence depletion technique, the vibrational structure of the upper electronic state ($A\ ^2\Pi_g$) was determined.[1,2] On the other hand, the dispersed fluorescence spectrum indicated vibrational structure in the ground electronic state ($X\ ^2\Pi_u$).[1] Out of the scope of previous analyses were bending vibrations, and the issue of possible couplings between bending vibrations and electronic motion, and spin–orbit coupling, which are of importance for an open-shell species with degenerate Π electronic states that contains sulfur atoms. In the present analysis, the spin–orbit splitting in the ground and the first excited state were examined, and the vibronic spectrum in the ground electronic state was investigated by applying the method for combined treatment of vibronic and spin––orbit interactions that was developed by Perić for a general *n*-atomic system,[4] and implemented in a Python program by Mitić *et al*. to calculate energies variationally.[5]

The employed computational methods are detailed in the following section Computational methods, after which the results and discussion are given in detail for the ground electronic state. The present conclusions and general outlook are given in the last section. Detailed data obtained as results of computations are placed in the Supplementary material to this paper.

COMPUTATIONAL METHODS

The electronic energy of the $X\ ^2\Pi_u$ ground state of the title molecule was calculated using the multi-reference configuration interaction (MRCISD) method[6,7] in its explicitly-correlated F12 variant,[8] within the framework of the Born–Oppenheimer approximation, using the MOLPRO 2012.1 quantum chemical software package.[9,10] In all calculations, the equilibrium nuclear geometry of the ground electronic state, *i.e.*, r_{S1C1} = 1.6358 Å, r_{C1C2} = 1.2571 Å and r_{C2S2} = 1.6358 Å, and the equilibrium geometry of the excited $A\ ^2\Pi_g$ state, *i.e.*, r_{S1C1} = 1.7172 Å, r_{C1C2} = 1.2300 Å and r_{C2S2} = 1.7172 Å, were used. These values were obtained in a previous work using the same MRCISD method.[1] Thus the approximation of fixed equilibrium internuclear distances during bending and stretching vibrations of the molecule was used. Two components of the Π_u degenerate electronic state, which splits during bending vibrations, were calculated within the D_{2h} subgroup of the $D_{\infty h}$ symmetry group at linear nuclear arrangements, and C_s point group symmetry (components A′ and A″) when molecule is bending at planar geometries, according to our model. Orbitals and states were also assigned within the C_{2v} and C_{2h} point group symmetries for *cis*- and *trans*-bending, respectively; In both cases, the *z*-axis is placed along the C_2 axis (in C_{2v}, the *yz*-plane was placed in the molecular plane, and in C_{2h} group – the *xy*-plane). Therefore, the Π_u state splits into A_1+B_1 states under *cis*--bending, and to A_u+B_u under *trans*-bending vibrational modes.

The reference function for the MRCI-F12 calculations was the complete active space self-consistent field (CASSCF) wavefunction,[11] obtained by (state-)averaging (SA) of two components of the ground state. The active space consists of $2\pi_u$, $2\pi_g$, $3\pi_u$, and $3\pi_g$ orbitals (actually, in the D_{2h} subgroup, the active space comprises $2b_{2u}$, $2b_{3u}$, $2b_{2g}$, $2b_{3g}$, $3b_{2u}$, $3b_{3u}$, $3b_{2g}$, and $3b_{3g}$ orbitals), where 11 electrons can be accommodated. Therefore, the method is abbreviated as SA-CAS(11,8). Other valence orbitals that are occupied in the ground state were set to be double-occupied ($5\sigma_g^+$, $6\sigma_g^+$, $7\sigma_g^+$, $5\sigma_u^+$, $6\sigma_u^+$). Upon bending, when the planar geometry of the nuclear framework (for both *cis*- and *trans*- bending modes) are set, the active

space consists of 16*a*′, 17*a*′, 18*a*′, 19*a*′, and 3*a*″, 4*a*″, 5*a*″, 6*a*″ molecular orbitals. The final used energy values were obtained by employing the internally contracted multi-reference configuration interaction method with single and double excitations (MRCISD)[6,7] in the F12 variant,[8] corrected with the additional perturbative Davidson cluster correction MRCI(Q), with relaxed reference. In the calculations of potential energy curves (PECs), the correlation-consistent polarized valence triple-zeta F12 (cc-pVTZ-F12) atomic basis set,[12] which is specially designed for explicitly correlated wavefunctions, was used. It is noted here that this basis set also has diffuse functions essential for calculations of anions. However, it was not necessary to add more diffuse basis functions due to the non-dipolar nature of the corresponding neutral (the neutral is unable to bind an additional electron to form a dipole-bound state, for which very diffuse functions in the basis set should be used).

The dependence of natural orbitals on the bending modes was calculated from the state-average CAS wavefunctions. Furthermore, harmonic frequencies were obtained using the single-reference coupled cluster RCCSD(T) method for open-shell species,[13] in the aug-cc--pVTZ and aug-cc-pVQZ basis sets,[14] by optimizing the one component of the degenerate ground state at strictly linear equilibrium geometry.

The spin–orbit (SO) splitting was calculated by diagonalization of the Breit–Pauli Hamiltonian in the basis of CASSCF wavefunctions, within the framework of the MRCI program,[15] for both the ground and excited $A\ ^2\Pi_g$ states at the equilibrium nuclear geometries of both states in question. Specifically, the SO Hamiltonian was diagonalized in the basis of two components of the ground state to obtain the spin–orbit splitting of the isolated ground state (in the D_{2h} symmetry group, these components are $1\ ^2\Pi_{B2u}$ and $1\ ^2\Pi_{B3u}$), and additionally in the basis of four components of both states ($1\ ^2\Pi_{B2u}$, $1\ ^2\Pi_{B3u}$, $1\ ^2\Pi_{B2g}$ and $1\ ^2\Pi_{B3g}$) in order to evaluate the influence of the excited state on the SO splitting in the ground state. All calculations of the SO states were carried out using the standard aug-cc-pVTZ basis set.[14]

In the following, the method used for the calculations of the vibronic levels in the ground electronic state of the $^{32}S^{12}C^{12}C^{32}S^-$ molecule is described. In order to investigate the Renner–Teller (RT) effect in the $X\ ^2\Pi_u$ electronic state of $SCCS^-$,[16] the variational approach was employed for the *ab initio* handling of combined effects of the Renner–Teller effect and spin–orbit coupling in tetra-atomic molecules with linear equilibrium geometry, which is described in details elsewhere.[17-28] The simple model is based on the assumption that the stretching vibrations and end-over-end rotations are separable from the degrees of freedom that are not directly involved in the vibronic coupling, namely electronic motion, bending vibrations and rotation about the axis *a* (= *z*) corresponding to the smallest moment of inertia. Since the low-lying vibronic levels of a symmetric type of molecule with linear equilibrium geometry are being calculated, the kinetic energy operator for infinitesimal vibrations in terms of *trans* and *cis* curvilinear symmetry coordinates was employed in order to obtain the force constants k_T, k_C, and the Renner–Teller parameters, ε_T and ε_C, from the *ab initio* calculated one-dimensional cuts of the potential surfaces and at bond lengths maintained at their equilibrium values. In this case, the spin–orbit operator is assumed in the phenomenological form:

$$\hat{H} = A_{SO}\hat{L}_z\hat{S}_z$$

where the value for the spin–orbit coupling constant (A_{SO}) obtained from previously described calculations of spin–orbit splitting in the ground state was used.

The reliability of the model applied in the present study was analyzed,[29] whereby special attention was paid to the topological structure of the adiabatic potential surfaces and non-adiabatic matrix elements in case of tetra-atomic molecules.[29,30] A perturbative and variational

approach for handling the Renner–Teller effect combined with spin–orbit coupling was also developed for symmetric five-atomic,[5,31] and six-atomic molecules with linear equilibrium geometry,[32,33] and at the end for molecules with an arbitrary number of nuclei.[4,5] The program for the variational treatment of the Renner–Teller effect in tetra-atomic molecules was written in the Python programming language using the Numpy package. Normal coordinates were assumed for the vibrational part of the Hamiltonian, which also allows the treatment of asymmetric types of molecules.

The vibronic basis for the variational calculation consisted of the direct product of the electronic wavefunction and the eigenfunction of a two-dimensional isotropic harmonic oscillator (Eq. (48) in Ref. 28) with $v_T \equiv v_4 \leq 15$, $v_C \equiv v_5 \leq 15$, $l_T \equiv l_4 \leq 15$ and $l_C \equiv l_5 \leq 15$, where v_T, v_C, l_T and l_C denote vibrational quantum numbers for *trans*-bending, *cis*-bending mode, and quantum numbers for *trans* and *cis*-bending angular momenta, respectively. The basis of such dimensions ensures full convergence of the computer for low-lying vibronic energy levels. The constructed vibronic Hamiltionian matrices (of dimensions about 1400×1400) were diagonalized using the Lanczos algorithm.[34,35]

RESULTS AND DISCUSSION

The $SCCS^-$ is a chemical species with an odd number of electrons (45 electrons), which has the ground electronic state of linear Π symmetry that splits upon bending into two electronic states of very similar energy. The electronic configuration is: $\ldots(2\pi_u)^4\ (2\pi_g)^4\ (3\pi_u)^3\ (3\pi_g)^0$, where only the system of π-orbitals that influence the order of low-lying electronic states, and comprises the active space in CASSCF calculations is shown. At linearity, this molecule has seven vibrational modes, three stretching (ν_1, ν_2, ν_3) and two degenerate bending modes, of which one is the *trans* (ν_4) and the other the *cis* mode (ν_5).

In order to calculate vibronic (vibrational-electronic) energies in this state, first the splitting of electronic energies upon bending vibrations have to be analyzed, calculated in the framework of Born–Oppenheimer approximation, then the spin–orbit splitting, because the presence of sulfur atoms indicates a strong coupling in this case. The bending potential curves (PECs) along the *cis*- and *trans*-bending coordinates ρ_C and ρ_T, respectively, defined as $\rho = 180° - \angle S–C–C$, are displayed in Fig. 1 (*ab initio* energies are presented in the Supplementary material, Tables S-I and S-II); the curves were obtained by fixing the internuclear distances at the equilibrium linear geometry of the ground state (see the Computational methods section). The most prominent feature of these splittings is the very small Renner–Teller effect along the *cis*-bending mode, and significant coupling in the *trans*-bending mode of vibration, which influence the vibronic spectra of this species, as will be seen later.

The energies of molecular (natural) orbitals upon *cis*- and *trans*-bending coordinates are depicted in Fig. 2 (energy values are shown in Tables S-III and S-IV). The highest occupied molecular orbital (HOMO) is the $3\pi_u$ orbital that splits upon *cis*- and *trans*-bending to $a_1 + b_1$ and $a_u + b_u$ orbitals, respectively, and has three electrons accommodated. The lowest-lying unoccupied molecular

orbital (LUMO) is the $3\pi_g$ orbital, lying relatively high in energy with respect to the HOMO (about +0.4 a.u., where a.u. is the abbreviation for atomic units of energy, Hartree). The energy of the $2\pi_g$ orbital, occupied with four electrons in the ground state, is more closely placed to the HOMO than the $3\pi_g$ orbital and hence, the first excited electronic state should emerge from the $2\pi_g \rightarrow 3\pi_u$ excitation, having now the electronic configuration of: $\ldots(2\pi_u)^4\ (2\pi_g)^3\ (3\pi_u)^4\ (3\pi_g)^0$, and indeed the $A\ ^2\Pi_g$ state was detected as the first excited state by fluorescence spectroscopy.[1,2]

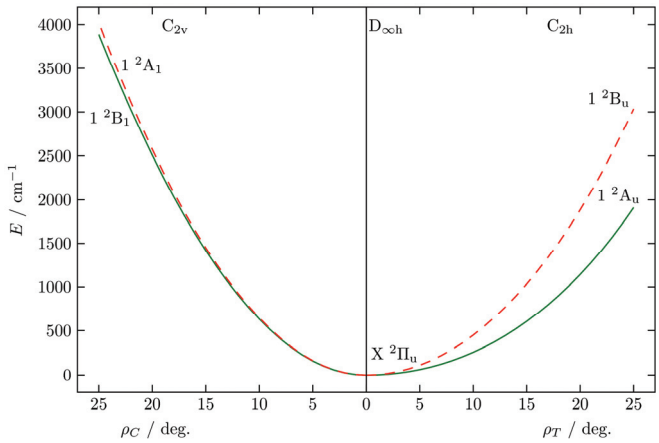

Fig. 1. The potential energy curves of the ground $X\ ^2\Pi_u$ state along the *cis*- (on the left-hand side) and *trans*-bending (right-hand side) coordinates, calculated by the state-average CASSCF(11,8)-MRSDCI(Q)-F12 method in the cc-pVTZ-F12 basis set. See main text for further details.

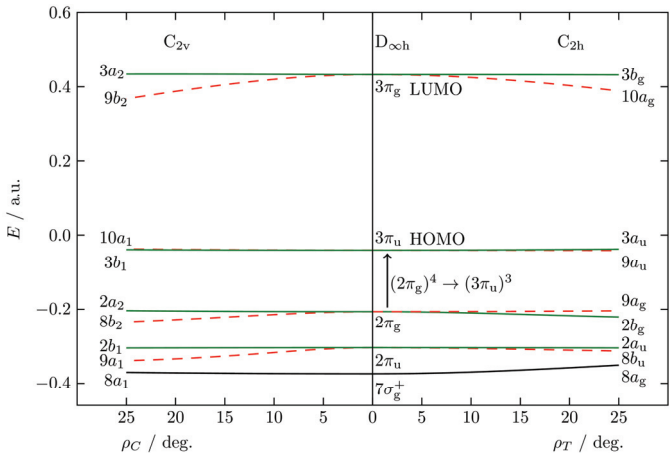

Fig. 2. Energy of molecular orbitals of $SCCS^-$ in the ground $X\ ^2\Pi_u$ state along the *cis*- (ρ_C) and *trans*-bending (ρ_T) coordinates, calculated by the state-average CASSCF(11,8) method in the cc-pVTZ-F12 basis set.

The *ab initio* computed frequencies of vibrational modes are outlined in Table I together with previous results. For stretching vibrations, the present values could be compared with previous theoretical and experimental results; the values obtained by using RCCSD(T)/aug-cc-pVTZ method are in accord with experimental frequencies, especially for the S–C stretching mode. For a degenerate vibration, the same frequencies (equal energy) were not obtained because of the RT effect, particularly for the *trans*-bending mode of vibration. Using the following equation for calculating the average frequencies:

$$\omega = \sqrt{\frac{k}{\mu}} = \sqrt{\frac{k' + k''}{2\mu}} = \frac{1}{\sqrt{2}}\sqrt{\omega'^2 + \omega''^2} \quad (1)$$

from ω' and ω'' values (higher and lower values of the same bending vibration), average values of ω_4 = 398.02 (403.21) cm^{-1} and ω_5 = 174.17 (173.70) cm^{-1} were obtained for *trans*- and *cis*-vibrations, respectively (see Table I), which are the *ab initio* computed values for these two bending vibrations. Additionally, the bending frequencies were calculated by using the model for the RT effect (further in the text), with the input parameters extracted from the bending potential energy curves (displayed in Fig. 1) up to 20°. The values of ω_4 = 412.56 cm^{-1} and ω_5 = 173.49 cm^{-1} were obtained. As could be noticed from Table I, there have hitherto been no reported values for the bending frequencies and therefore, the present values could not be compared with previous results. Nevertheless, the frequencies obtained from the present RT model will be compared with experimental frequencies in the further discussion.

TABLE I. Vibrational frequencies (cm^{-1}) of $SCCS^-$ in the $X\,^2\Pi_u$ state (see main text for further details)

Method	Vibrational frequency				
	ν_1 (σ_g) (C–C stretching)	ν_2 (σ_g) (S–C stretching)	ν_3 (σ_u) (asymmetric stretching)	ν_4 (π_g) (*trans*-bending)	ν_5 (π_u) (*cis*-bending)
RCCSD(T)/ aug-cc-pVTZ	2008.61	501.44	1037.82	398.02 [339.91, 448.66]	174.17 [173.23, 175.10]
RT model				412.56[a]	173.49[a]
RCCSD(T)/ aug-cc-pVQZ	2013.24	505.56	1047.57	403.21 [346.20, 453.10]	173.70 [172.72, 174.67]
CCSD(T)/ aug-cc-pVTZ	2014[b]	500[b]	1043[b]	/	/
MRCI/ aug-cc-pVTZ	2037[b]	507[b]	1047[b]		
Experimental	1971.53[c]	502.58[c]	/	/	/

[a]This work, from the MRCI(Q)/cc-pVTZ-F12 bending potential curves; [b]calculated values of stretching modes;[1] [c]effective vibrational constants determined from the LIF spectrum[1]

As the title anion possesses sulfur atoms, relatively strong spin–orbit coupling could be expected, with splittings similar in energies to the bending vibrations. In this case, the molecule has two spin–orbit components, one with $\Omega = = \pm 3/2$ and the other with $\Omega = \pm 1/2$, where Ω is the quantum number equal to $\Lambda+\Sigma$ (Λ is the quantum number of the electronic orbital angular momentum along the axis of the molecule; Σ is the quantum number of the projection of the total electronic spin angular momentum onto the same axis); $\Lambda = \pm 1$ for the Π state, and $\Sigma = \pm 1/2$ for a doublet, therefore Ω can have values of 3/2, 1/2, –1/2 and –3/2, giving rise to two degenerate spin–orbit components: $^2\Pi_{u3/2}$ and $^2\Pi_{u1/2}$ in the $X\ ^2\Pi_u$ state. From the electronic configuration, it could be deduced that this state is inverted and therefore, the $^2\Pi_{u3/2}$ should be lower in energy than the $^2\Pi_{u1/2}$ component. The present calculations (see Computational methods section) confirmed that two spin–orbit components in the ground state are separated by about 250 cm^{-1}, as will be shown below.

The SO coupling constant (A_{SO}) for the (isolated) $X\ ^2\Pi_u$ state is –243.31 cm^{-1}, where the minus sign comes from the inverted state. The same holds for the isolated $A\ ^2\Pi_g$ state, with an SO splitting of 298.57 cm^{-1} ($A_{SO} = –298.57\ cm^{-1}$). In order to incorporate the influence of the higher lying $A\ ^2\Pi_g$ state onto the SO coupling in the ground state, the A state was also added in the spin–orbit matrix. Therefore, the spin–orbit eigenvalues and eigenstates for both states under consideration are obtained by diagonalizing the Breit–Pauli spin–orbit operator in the basis of all four components of the $X\ ^2\Pi_u$ and $A\ ^2\Pi_g$ states (see Computational methods section).

The SO splitting of the lower and the upper state at: a) linear equilibrium geometry of the ground state, and b) at linear equilibrium geometry of the excited state, which is essential for comparing with experimental results, is presented in Fig. 3. Namely, in the reported dispersed fluorescence spectrum,[1] the vibronic states of the ground state are populated by the fluorescence from the lowest-lying energy level in the excited state. As could be seen in Fig. 3, at the excited state equilibrium geometry, the ground state is higher in energy by 2035 cm^{-1}, and the excited state is lower by 1785 cm^{-1} than the same states at the geometry of the ground state. Nevertheless, the splittings of the spin–orbit components do not change significantly. The vertical excitation energy of the $A\ ^2\Pi_g$ state is 20864 cm^{-1} at the ground state geometry and 17044 cm^{-1} at its own geometry. These values can be compared with the band origin 0_0^0 value of 18423.99 cm^{-1},[1] and it could be concluded that the band origin is in between the two values. (In order to calculate the band origin frequency, the zero-point vibrational energy (ZPVE) correction should be included; however, it was assumed here that this correction is similar for both states in question). Note that the experimental information available for the ground state was obtained from the radiative decay process from the excited to the ground state, which obviously correspond more to the nuclear geometry of the excited state.

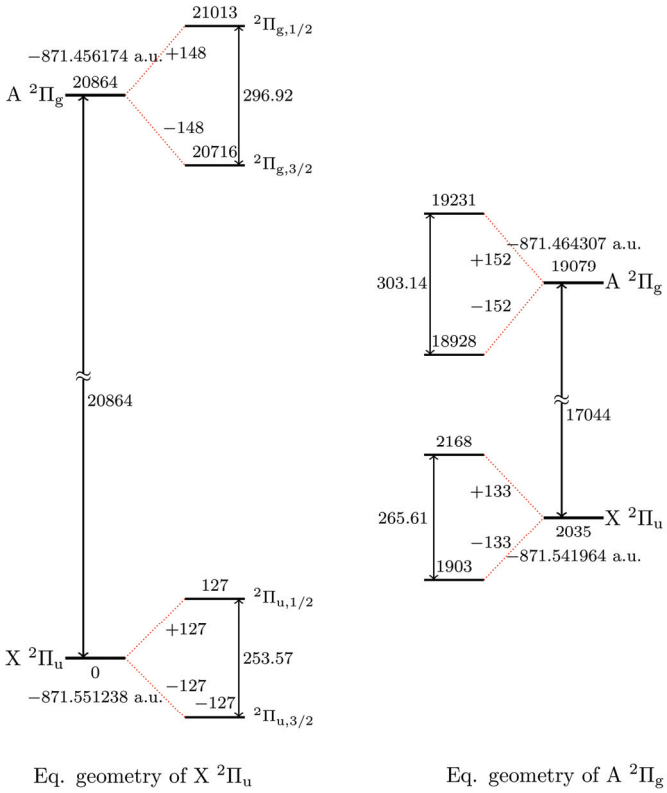

Fig. 3. Scheme of the spin–orbit splitting in the $X\,^2\Pi_u$ and $A\,^2\Pi_g$ states at the equilibrium geometry of both states under consideration. Note: Zero energy corresponds to the electronic energy of the $X\,^2\Pi_u$ state without SO splitting.

From Fig. 3, it is also evident that when adding the excited state into calculations, the SO constant for the ground state changes from –243.31 to –253.56 cm^{-1}. On the other hand, the A_{SO} for the isolated $A\,^2\Pi_g$ state is nearly the same (–298.57 cm^{-1}) as in this case, with a value of –296.61 cm^{-1}, only 2 cm^{-1} smaller.

Furthermore, in order to investigate the probability of transitions amongst different spin–orbit components (under electric dipole interaction), the transition dipole moment (R_{mn}) between all electronic spin–orbit components are also calculated, and the results for $^2\Pi_{g3/2}\rightarrow{}^2\Pi_{u3/2}$ and $^2\Pi_{g3/2}\rightarrow{}^2\Pi_{u1/2}$ transitions are presented in Table II. The square of the transition dipole moment from the initial state m to the final state n is proportional to the transition intensity, and was calculated from the formula:

$$R_{nm}{}^2 = \sum_{i,k} \sum_{\alpha=x,y,z} \left| R_\alpha{}^{n_i,m_k} \right|^2 \tag{2}$$

where $R_\alpha^{ni,mk}$ are the transition matrix elements, and i and k denote the degenerations of n,m levels (equal two for all spin–orbit components). As could be expected from the transition rules, only fluorescence from 3/2 to 3/2, or from 1/2 to 1/2 are allowed at linearity. However, upon bending, when the potential energy curves split and the symmetry of the molecule breaks from linear to the C_{2v} or C_{2h} symmetry group, then such forbidden transitions becomes vibronically allowed. Accordingly, at 10°, the value of R_{mn}^2 between the 3/2 and the 3/2 component is 1 Debye* and 3.6 Debye at *cis* and *trans*-bending, respectively (see Table II), rather small compared to the main $^2\Pi_{g3/2}\rightarrow{}^2\Pi_{u3/2}$ transition; Yet, at 20°, the transition dipole moments are almost the same, and for 25°, the dominant transitions are between different $|\Omega|$ components. Consequently, based on these findings, the transition $^2\Pi_{g3/2}\rightarrow{}^2\Pi_{u1/2}$ could in principle occur and be detected experimentally, if the bending vibrations are excited.

TABLE II. The square of the transition dipole moment (in D) between spin–orbit components in respect to bending angles. See main text for details

Bending angle, °	Transition			
	$^2\Pi_{g3/2}\rightarrow{}^2\Pi_{u3/2}$	$^2\Pi_{g3/2}\rightarrow{}^2\Pi_{u1/2}$	$^2\Pi_{g3/2}\rightarrow{}^2\Pi_{u3/2}$	$^2\Pi_{g3/2}\rightarrow{}^2\Pi_{u1/2}$
	cis-Bending		*trans*-Bending	
0	22.084	0.000	22.084	0.000
5	21.901	0.066	21.729	0.357
10	20.595	1.010	18.527	3.560
15	16.678	4.295	14.129	7.952
20	10.212	9.830	10.195	11.868
25	4.477	14.318	6.371	15.658

As the illustration of the magnitude of the splittings of the electronic energy upon bending, a) when SO coupling is neglected, and b) by taking into account the SO coupling, the electron energy splittings from 0 up to 25° are presented , in Fig. 4 for the *cis*-bending (the upper panel), and *trans*-bending mode (lower panel). Obviously, in line with Fig. 1, at *cis*-bending vibrations, the splitting is small, from 3.4 up to 67 cm^{-1} at 5 and 20°, respectively. Simultaneously, at *trans*-bending of the molecule, the PEC splits from 49 up to the 743 cm^{-1}, showing also that upon *trans*-bending, the Renner–Teller effect will be strong and that the splitting of the lines and rather complicated vibronic spectra upon *trans*-bending ν_4 excitation could be expected. The SO splitting is largest at linearity, and then upon bending its effect is to move the energies of the higher state up and the energy of the lower state down, but this effect gradually decrease with enhancement of the bending angles.

Finally, now the vibronic levels calculated by employing the model for the combined treatment of the Renner–Teller and spin–orbit couplings (see Comput-

* 1 Debye = 3.33564×10^{-30} C m

ational methods section) are presented. By fitting the mean potential and half the difference between *ab initio* calculated adiabatic potentials (depicted in Fig. 1), the force constants k_T, k_C and Renner–Teller parameters, ε_T and ε_C, were calculated (*via*, *e.g.*, Eq. (32) and (33) in Ref. 29) and their values are: $k_T = 0.1107366$, $k_C = 0.1902430$, $\varepsilon_T' = 0.0281897$, and $\varepsilon_C' = 0.0022725$, in units Hartree rad^{-2}; these force constants and Renner–Teller parameters are defined in terms of curvilinear symmetry coordinates. They can be easily transformed to those in terms of normal coordinates (*e.g.*, Refs. 19, 28, 29), to obtain $\omega_T \equiv \omega_4 = 412.563$ cm^{-1}, $\omega_C \equiv \omega_5 = 173.494$ cm^{-1}, $\varepsilon_T \equiv \varepsilon_4 = 0.254565$, and $\varepsilon_C \equiv \varepsilon_5 = 0.011945$, where Renner–Teller parameters are now dimensionless. Defined in terms of normal coordinates, these constants can be compared to the *ab initio* obtained frequencies (see Table I), and along with the spin–orbit coupling constant of –253.56 cm^{-1} are used as the input parameters for the computer program.

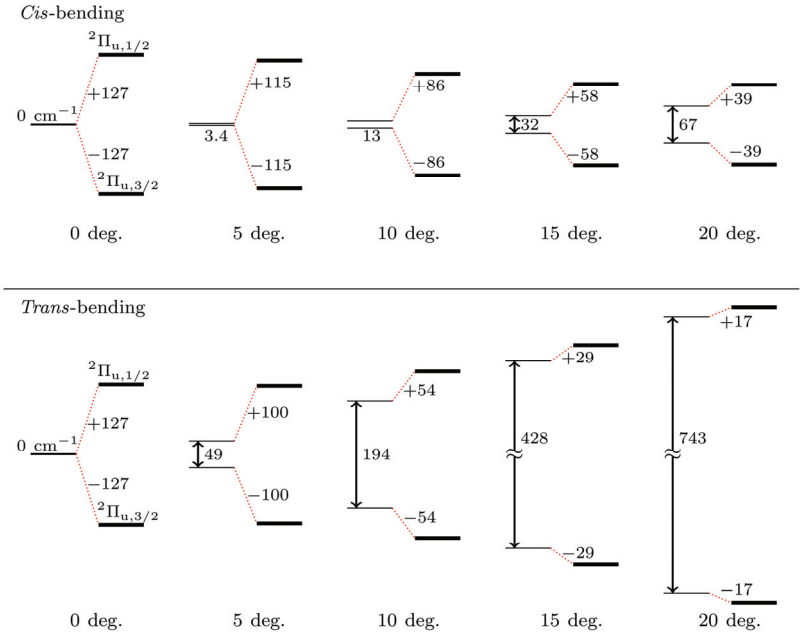

Fig. 4. Illustrations of the splitting of the $X\,^2\Pi_u$ electronic energy state upon *cis*- and *trans*-bending and spin–orbit coupling.

It is assumed that the quantum numbers $K = l + \Lambda$ and $P = K + \Sigma$ corresponding to the *z*-component of the vibronic angular momentum excluding and including spin, respectively, are good quantum numbers ($l = l_4 + l_5$ is the quantum number for the vibrational bending angular momentum, Λ for electronic orbital, and Σ for spin angular momentum along the molecular axis). Additionally, as stated previously, the quantum number Ω in this case is also a good quantum

number and hence, the equality $P = K + \Sigma = l + \Lambda + \Sigma = l + \Omega$ can be equally written, where strictly speaking only the quantum number of the total angular momentum, P, is the good quantum number. Due to this, the treatment of the Renner–Teller effect could be carried out separately within a particular K and P (*i.e.*, Σ) subspace. In the present work, K, Λ, l, Σ, Ω and P were considered signed quantities, but because vibronic levels with $|K| \neq 0$ (and $|P| \neq 0$) are in the applied model always doubly degenerate, only nonnegative values for K were calculated. The symmetry of the vibronic levels is determined by the direct product of the electronic, *trans*- and *cis*-bending species, *i.e.*, in the case of a Π_u electronic state, the total symmetry will be of $\Pi_u \times (\Pi_g)^{v^T} \times (\Pi_u)^{v^C}$ symmetry and therefore, the vibronic states are of *g*-type symmetry if the vibrational quantum number for *cis*-bending mode, ν_C, is odd and are of *u*-type if ν_C is even. The situation is opposite for the electronic state with *g*-type symmetry ($A\ ^2\Pi_g$ state). $K = 0$ vibronic levels, *i.e.*, Σ levels (not to be mixed with the quantum number Σ), can be characterized additionally with + or – according to their symmetry with respect to σ_v reflection. Therefore, calculated vibronic states are labeled as $^{2S+1}K_{|P|,u/g}$.

A list of low-lying energy levels and their energies are given in Table III for $X\ ^2\Pi_{u3/2}$ (and in Table S-5 for $X\ ^2\Pi_{u1/2}$) spin–orbit component of the ground state.

Now, the vibronic levels presented in Table III were analyzed. When only the *cis*-bending mode is excited (*e.g.*, in $\nu_4\nu_5$ = 01, 02, 03, 04,…), there is no splitting of the energy according to different l_5 or K values and consequently, the Renner–Teller effect is negligible and inactive in these cases. On the contrary, when only the *trans*-bending mode is excited (in $\nu_4\nu_5$ = 10, 20,…), the splitting of $l_4 = +1$ and –1 levels is 28.3 cm^{-1} for 10, and between $l_4 = +2$ and –2 levels, it is 38.3 cm^{-1} for 20 excitation, which is the consequence of the relatively strong Renner–Teller effect in the *trans*-bending mode. In combined excitations (11, 12, 13, 21,…), the levels are grouped according to different l_4 values. The same conclusion is also valid for the other spin–orbit component (see Table S-5).

Now, the possible transitions from the lowest-lying vibronic level in the excited $A\ ^2\Pi_g$ state (in the $\Omega = \pm 3/2$ spin–orbit component of this state), labeled as $1\ ^2\Pi_{3/2g}$, to the various vibronic levels in the ground state could be examined, in order to possibly assign the unassigned lines in the disperse fluorescence spectrum recorded for $SCCS^-$ species (Table IV, Ref. 1). When the molecule is linear, the only possible transition from the $1\ ^2\Pi_{3/2g}$ vibronic state, according to Table II, is to the vibronic levels in the lowest 3/2 spin–orbit component of the ground state (*i.e.*, the transition $^2\Pi_{g3/2} \rightarrow {}^2\Pi_{u3/2}$). Furthermore, due to parity forbidden $g \rightarrow g$ transition, the fluorescence is possible only to *ungerade* (*u*) vibronic levels in the ground state. Subsequently, in the dispersed fluorescence spectra, one

can see in principle the *trans*-bending excitations and only even *cis*-bending excitations in the ground electronic state. Additionally, the operative selection rules

TABLE III. The low-energy vibronic levels in the $X\ ^2\Pi_{u3/2}$ component of the ground state of $SCCS^-$. ΔE is relative energy in respect to the lowest vibronic level $1\ ^2\Pi_{3/2u}$; the $^2\Pi_{3/2u}$ levels are marked in bold. See main text for further details

$\Omega = \pm 3/2$ ($\Lambda = 1$ and $\Sigma = 1/2$, or $\Lambda = -1$ and $\Sigma = -1/2$)									
$\nu_4\nu_5$	$\nu_4 l_4 \nu_5 l_5 \Lambda$	$^{2S+1}K_{\lvert P\rvert,u/g}$	E cm^{-1}	ΔE cm^{-1}	$\nu_4\nu_5$	$\nu_4 l_4 \nu_5 l_5 \Lambda$	$^{2S+1}K_{\lvert P\rvert,u/g}$	E cm^{-1}	ΔE cm^{-1}
00	00001	**$1\ ^2\Pi_{3/2u}$** [a]	454.0	0.0	13	11331	$^2H_{11/2g}$	1376.5	922.5
01	00111	$^2\Delta_{5/2g}$	627.5	173.5		11311	$^2\Phi_{7/2g}$	1376.6	922.6
	001–11	$^2\Sigma^-_{1/2g}$	627.5	173.5		113–11	$^2\Pi_{3/2g}$	1376.6	922.6
	0011–1	$^2\Sigma^+_{1/2g}$	627.5	173.5		113–31	$^2\Pi_{1/2g}$	1376.7	922.7
02	00221	$^2\Phi_{7/2u}$	801.0	347.0	21	20111	$^2\Delta_{5/2g}$	1374.8	920.8
	00201	**$^2\Pi_{3/2u}$**	801.0	347.0		201–11	$^2\Sigma^-_{1/2g}$	1374.8	920.8
	002–21	$^2\Pi_{1/2u}$	801.0	347.0		20–111	$^2\Sigma^+_{1/2g}$	1374.8	920.8
10	1–1001	$^2\Sigma^-_{1/2u}$	827.8	373.8		2–21–11	$^2\Delta_{3/2g}$	1388.2	934.2
	1100–1	$^2\Sigma^+_{1/2u}$	827.8	373.8		2–2111	$^2\Sigma^-_{1/2g}$	1388.3	934.3
	11001	$^2\Delta_{5/2u}$	856.1	402.1		221–1–1	$^2\Sigma^+_{1/2g}$	1388.3	934.3
03	00331	$^2\Gamma_{9/2g}$	974.5	520.5		221–11	$^2\Delta_{5/2g}$	1426.5	972.5
	00311	$^2\Delta_{5/2g}$	974.5	520.5		22111	$^2\Gamma_{9/2g}$	1426.4	972.4
	003–11	$^2\Sigma^-_{1/2g}$	974.5	520.5	06	00661	$^2K_{15/2u}$	1494.9	1040.9
	0031–1	$^2\Sigma^+_{1/2g}$	974.5	520.5		00641	$^2H_{11/2u}$	1494.8	1040.8
	003–31	$^2\Delta_{3/2g}$	974.5	520.5		00621	$^2\Phi_{7/2u}$	1494.8	1040.8
11	1–1111	$^2\Pi_{3/2g}$	1001.3	547.3		00601	**$^2\Pi_{3/2u}$**	1494.8	1040.8
	1–11–11	$^2\Pi_{1/2g}$	1001.3	547.3		006–21	$^2\Pi_{1/2u}$	1494.9	1040.9
	11111	$^2\Phi_{7/2g}$	1029.6	575.6		006–41	$^2\Phi_{5/2u}$	1495.0	1041.0
	111–11	$^2\Pi_{3/2g}$	1029.6	575.6		006–61	$^2H_{9/2u}$	1495.2	1041.2
04	00441	$^2H_{11/2u}$	1148.0	694.0	14	1–1441	$^2\Gamma_{9/2u}$	1521.7	1067.7
	00421	$^2\Phi_{7/2u}$	1147.9	693.9		1–1421	$^2\Delta_{5/2u}$	1521.6	1067.6
	00401	**$^2\Pi_{3/2u}$**	1147.9	693.9		1–1401	$^2\Sigma^-_{1/2u}$	1521.6	1067.6
	004–21	$^2\Pi_{1/2u}$	1148.0	694.0		1140–1	$^2\Sigma^+_{1/2u}$	1521.6	1067.6
	004–41	$^2\Phi_{5/2u}$	1148.1	694.1		1–14–21	$^2\Delta_{3/2u}$	1521.7	1067.7
12	1–1221	$^2\Delta_{5/2u}$	1174.7	720.7		1–14–41	$^2\Gamma_{7/2u}$	1521.8	1067.8
	1–1201	$^2\Sigma^-_{1/2u}$	1174.7	720.7		11441	$^2I_{13/2u}$	1550.0	1096.0
	1120–1	$^2\Sigma^+_{1/2u}$	1174.7	720.7		11421	$^2\Gamma_{9/2u}$	1550.0	1096.0
	1–12–21	$^2\Delta_{3/2u}$	1174.8	720.8		11401	$^2\Delta_{5/2u}$	1550.1	1096.1
	11221	$^2\Gamma_{9/2u}$	1203.1	749.1		114–21	$^2\Sigma^-_{1/2u}$	1550.2	1096.2
	11201	$^2\Delta_{5/2u}$	1203.1	749.1		1–142–1	$^2\Sigma^+_{1/2u}$	1550.2	1096.2
	112–21	$^2\Sigma^-_{1/2u}$	1203.1	749.1		114–41	$^2\Delta_{3/2u}$	1550.3	1096.3
	1–122–1	$^2\Sigma^+_{1/2u}$	1203.1	749.1	22	202–21	$^2\Pi_{1/2u}$	1548.2	1094.2
20	20001	**$^2\Pi_{3/2u}$**	1201.3	747.3		20201	**$^2\Pi_{3/2u}$**	1548.2	1094.3
	2–2001	$^2\Pi_{1/2u}$	1214.7	760.7		20221	$^2\Phi_{7/2u}$	1548.3	1094.3
	22001	$^2\Phi_{7/2u}$	1253.0	799.0		2–22–21	$^2\Phi_{5/2u}$	1561.7	1107.7
05	00551	$^2I_{13/2g}$	1321.4	867.4		2–2201	$^2\Pi_{1/2u}$	1561.8	1107.8
	00531	$^2\Gamma_{9/2g}$	1321.4	867.4		2–2221	**$^2\Pi_{3/2u}$**	1561.8	1107.8

00511	$^2\Delta_{5/2g}$	1321.4	867.4	22221	$^2H_{11/2u}$	1599.9	1145.9
005–11	$^2\Sigma_{1/2g}^-$	1321.4	867.4	22201	$^2\Phi_{7/2u}$	1599.9	1145.9
0051–1	$^2\Sigma_{1/2g}^-$	1321.4	867.4	222–21	$\mathbf{^2\Pi_{3/2u}}$	1598.9	1144.9

TABLE III. Continued

$\Omega = \pm 3/2$ ($\Lambda = 1$ and $\Sigma = 1/2$, or $\Lambda = -1$ and $\Sigma = -1/2$)				
$\nu_4\nu_5$	$\nu_4 l_4 \nu_5 l_5 \Lambda$	$^{2S+1}K_{\lvert P\rvert,u/g}$	E cm^{-1}	ΔE cm^{-1}
05	005–31	$^2\Delta_{3/2g}$	1321.5	867.5
	005–51	$^2\Gamma_{7/2g}$	1321.6	867.6
13	1–1331	$^2\Phi_{7/2g}$	1348.2	894.2
	1–1311	$^2\Pi_{3/2g}$	1348.1	894.1
	1–13–11	$^2\Pi_{1/2g}$	1348.2	894.2
	1–13–31	$^2\Phi_{5/2g}$	1348.3	894.3

are $\Delta K = \Delta P = 0$ in the levels in which one or more bending modes are excited (see *e.g.*, Ref. 36), therefore transitions to the $^2\Pi_{3/2u}$ vibronic states in the ground state (marked bold in Table III) are expected.

In the dispersed fluorescence experiment in which the analyzed spectrum was recorded, the excitation laser frequency was set to a fixed value of 18423 cm^{-1}, which is the frequency of the origin band assigned by rotationally resolved LIF excitation spectrum (the band 0_0^0).[1] Upon fluorescence from the initial 1 $^2\Pi_{3/2g}$ level, the transition frequencies to the final states in the ground state have lower values, depending, of course, on the relative energies of the levels in respect to the ground 1 $^2\Pi_{3/2u}$ level. Therefore, this experimental setup enables direct energy determination of the vibronic levels in the ground state to which the transitions are allowed. Most of the bands in the recorded spectrum are progressions with ≈500 cm^{-1} separation. This frequency was assigned to the fundamental vibration of the v_2 stretching mode (see also Table I), with the effective value of $\omega_2 = 502.58$ cm^{-1}.[1] No pure bending modes below this value were detected. However, there were some bands with positions above 500 cm^{-1} from the origin band that are of low intensity and that could be assigned according to the obtained results. Namely, it could be seen in Table III that the first excited $^2\Pi_{3/2u}$ vibronic state is 347.0 cm^{-1} above the lowest vibronic state, which corresponds to the second overtone of the *cis*-bending vibration ($\nu_4\nu_5$ = 02). In the spectrum, one band was moved by 849 cm^{-1} from the origin, which could be assigned, according to the results in this work, as the band $2_1^0 5_2^0$, *i.e.*, as the combined excitation of the ν_2 mode (with a frequency for 2_1^0 of 501 cm^{-1}) and ν_5 mode (348 cm^{-1}), Indeed, the value of 348 cm^{-1} is in very good agreement with the in this work obtained value of 347.0 cm^{-1}. Furthermore, in Table III, the relative energy of the $^2\Pi_{3/2u}$ state obtained by the 20 excitation is 747.3 cm^{-1}, which corresponds to the second overtone of the *trans*-bending mode. This fre-

quency was associated to the detected 737 cm^{-1} band position in fluorescence spectrum and hence, this band could be assigned as 4_2^0. The third unassigned band in the dispersed spectrum was the band at 1236 cm^{-1} from the origin, which could be assigned to a combination band $2_1^0 4_2^0$, the combined ν_2 (501 cm^{-1}) and ν_4 (735 cm^{-1}) vibrational mode that would lie from the present calculations at a bit higher value of 1248.3 cm^{-1}. These and other possible assignments are presented in Table IV.

TABLE IV. Assignments of the bands recorded by the dispersed fluorescence spectroscopy by Nakajima *et al.*,[1] using vibronic levels calculated in this work

Band position[a], cm^{-1}	Vibronic state[b] ($v_4 l_4 v_5 l_5 \Lambda$) $^{2S+1}K_{\|P\|,u/g}$	ΔE[c] / cm^{-1}	Assignment[d]
0	(00001) 1 $^2\Pi_{3/2u}$	0	0_0^0 [a]
501	–	501	2_1^0 [a]
737	(20001) $^2\Pi_{3/2u}$	747 (+10)[e]	4_2^0
849	(00201) $^2\Pi_{3/2u}$	848	$2_1^0 5_2^0$
1003	–	1002	2_2^0 [a]
1236	(20001) $^2\Pi_{3/2u}$	1248 (+12)	$2_1^0 4_2^0$
1503	–	1503	2_3^0 [a]
1645	(222–21) $^2\Pi_{3/2u}$	1646 (+1)	$2_1^0 4_2^0 5_2^0$?
1727	(20001) $^2\Pi_{3/2u}$	1749 (+22)	$2_2^0 4_2^0$
1962	–	1962	1_1^0 [a]
2002	–	2004	2_4^0 [a]
2059	(20201) $^2\Pi_{3/2u}$	2096 (+37)	$2_2^0 4_2^0 5_2^0$?
2143	(222–21) $^2\Pi_{3/2u}$	2147 (+4)	$2_2^0 4_2^0 5_2^0$?
2200	(20001) $^2\Pi_{3/2u}$	2250 (+50)	$2_3^0 4_2^0$
2460	–	2463	$1_1^0 2_1^0$ [a]
2501	–	2505	2_5^0 [a]
2558	(20201) $^2\Pi_{3/2u}$	2597 (+39)	$2_3^0 4_2^0 5_2^0$
2957	–	2964	$1_1^0 2_2^0$ [a]
2996	–	3006	2_6^0 [a]
3052	(20201) $^2\Pi_{3/2u}$ or (2–2221) $^2\Pi_{3/2u}$	3056 (+4) 3070 (+18)	$1_1^0 4_2^0 5_2^0$
3159	(20001) $^2\Pi_{3/2u}$	3210 (+51)	$1_1^0 2_1^0 4_2^0$
3454	–	3465.0	$1_1^0 2_3^0$ [a]
3539	(20201) $^2\Pi_{3/2u}$	3557 (+18)	$1_1^0 2_1^0 4_2^0 5_2^0$
3900	–	3924	1_2^0 [a]
3949	–	3966	$1_1^0 2_4^0$ [a]

[a]From Ref.1; [b]in this column the bending vibronic states of the $X\,^2\Pi_u$ state of $SCCS^-$ (see Table III) involved in the transition are presented; [c]the relative energy ΔE is computed as the sum of the relative energy of a vibronic state obtained in this work (and shown in Table III) and stretching vibrations taken from the 2_1^0 and 1_1^0 bands, with the values fixed to: ω_1 = 1962 cm^{-1}, ω_2=501 cm^{-1}; [d]assignments followed by a question mark are questionable; [e]in parentheses, 3rd column, we show the deviations of calculated values from experimental band positions

According to the above assignments, the computed frequencies of the 4_2^0 and 5_2^0 bands are close to the experimental values, especially in the case of the *cis*-bending mode. The frequency for the *trans*-bending mode is somewhat higher

than the experimental one. However, when the input parameters for the program are changed, and the values for frequencies fitted from the potential curves up to $\rho = 15°$ (instead of 20°) are used, a value of 347.4 cm^{-1} is obtained for the 02 $^2\Pi_{3/2u}$ level, nearly equal to 347.0 cm^{-1} (see Table III), and for the 20 $^2\Pi_{3/2u}$ vibronic state, a relative energy of 730.3 cm^{-1} is obtained, lying closer to the experimentally determined value of 737 cm^{-1} than the calculated value of 747.3 cm^{-1} (Table III). Additionally, the *trans*-mode exhibits a pronounced anharmonicity because, for higher frequencies, the experimental values are significantly lower than expected from the developed model, which use a harmonic approximation.

CONCLUSIONS

Using the model for the Renner–Teller effect in any-atomic linear species developed by Perić and coworkers in its variational form,[5] the vibronic levels in the ground $X\ ^2\Pi_u$ state of $SCCS^-$ were calculated. It was demonstrated that the Renner–Teller effect is significant in the *trans*-bending mode of vibration, producing splitting of the excited bending levels into several components; on the contrary, it is inactive in the *cis*-bending mode. Accordingly, previously unassigned bands from the LIF spectrum were assigned. Furthermore, the spin–orbit splitting of the two components in the ground electronic state was calculated to be 253 cm^{-1}, being the reason for classifying the vibronic levels into different spin–orbit electronic components. On the account of relatively good agreement of the calculated vibronic levels with experimental data, the description of bending vibrations and the vibronic spectrum obtained in the current work could help in further experimental investigations and detection of the title species.

SUPPLEMENTARY MATERIAL

Detailed data obtained as results of computations are available electronically from http://www.shd.org.rs/JSCS/, or from the corresponding author on request.

Acknowledgements. The present research was supported by the ON172040 project of the Ministry of Education, Science, and Technological Development of the Republic of Serbia. Part of the *ab initio* calculations was realized using the HPC infrastructure Leo3e of the University of Innsbruck. On the occasion of the 70th birthday of Prof. emeritus Miljenko Perić, we express our appreciation and affection. We hope he will not be disappointed by the present modest implementation of his “simple” model.

ИЗВОД

$SCCS^-$ РАДИКАЛ: РЕНЕР–ТЕЛЕРОВ ЕФЕКАТ У ОСНОВНОМ ЕЛЕКТРОНСКОМ СТАЊУ

СТАНКА В. ЈЕРОСИМИЋ, МАРКО Љ. МИТИЋ и МИЛАН З. МИЛОВАНОВИЋ

Факултет за физичку хемију, Универзитет у Београду, Студентски трг 12–16, ПАК 105305, 11158 Београд

$SCCS^-$ је детектован помоћу ласерски индуковане флуоресцентне спектроскопије 2003. године (M. Nakajima, Y. Yoneda, Y. Sumiyoshi, T. Nagata, Y. Endo, *J. Chem. Phys.* **119** (2003) 7805), након чега је добијени спектар анализиран и резултати представљени

заједно са подацима добијеним помоћу *ab initio* израчунавања. Симетричне истежуће вибрације су асигниране и у основном $X\ ^2\Pi_u$ и у првом побуђеном $A\ ^2\Pi_g$ електронском стању, међутим нису објављени подаци о спин–орбитном цепању нити о савијајућим вибрационим модовима. У овом раду рачунати су вибронски нивои основног електронског стања $SCCS^-$ помоћу модела за третман Ренер–Телеровог ефекта у линеарним врстама са било којим бројем атома, који су развили Перић и сарадници у форми варијационог рачуна (M. Mitić, R. Ranković, M. Milovanović, S. Jerosimić, M. Perić, *Chem. Phys.* **464** (2016) 55), користећи притом *ab initio* методу вишереферентне интеракције конфигурација за добијање кривих потенцијалне енергије у Борн–Опенхајмеровој апроксимацији. Додатно, истраживано је спин–орбитно цепање у основном електронском стању узимајући у обзир интеракцију са првим побуђеним стањем, и објављене енергије добијене помоћу комбинованог третмана вибронске и спин–орбитне интеракције у основном стању. На крају, на бази садашњих резултата предложене су асигнације трака које нису биле асигниране у раду Nakajima *et al.*

(Примљено 1. априла, прихваћено 6. маја 2019)

REFERENCES

1. M. Nakajima, Y. Yoneda, Y. Sumiyoshi, T. Nagata, Y. Endo, *J. Chem. Phys.* **119** (2003) 7805 (https://doi.org/10.1063/1.1608844)
2. M. Nakajima, Y. Matsuyama, Y. Sumiyoshi, Y. Endo, *Chem. Phys. Lett.* **410** (2005) 172 (https://doi.org/10.1016/j.cplett.2005.05.058)
3. T. Maeyama, T. Oikawa, T. Tsumura, N. Mikami, *J. Chem. Phys.* **108** (1998) 1368 (https://doi.org/10.1063/1.475510)
4. M. Perić, *Mol. Phys.* **105** (2007) 59 (https://doi.org/10.1080/00268970601129076)
5. M. Mitić, R. Ranković, M. Milovanović, S. Jerosimić, M. Perić, *Chem. Phys.* **464** (2016) 55 (https://doi.org/10.1016/j.chemphys.2015.11.002)
6. H. Werner, P. Knowles, *J. Chem. Phys.* **89** (1988) 5803 (https://doi.org/10.1063/1.455556).
7. K. R. Shamasundar, G. Knizia, H. J. Werner, *J. Chem. Phys.* **135** (2011) 054101 (https://doi.org/10.1063/1.3609809)
8. T. Shiozaki, G. Knizia, H. J. Werner, *J. Chem. Phys.* **134** (2011) 034113 (https://doi.org/10.1063/1.3528720).
9. *MOLPRO, version 2012.1, a package of* ab initio *programs* (http://www.molpro.net)
10. H. J. Werner, P. J. Knowles, G. Knizia, F. R. Manby, M. Schütz, *Wiley Interdiscip. Rev. Comput. Mol. Sci.* **2** (2012) 242 (https://doi.org/10.1002/wcms.82)
11. H. Werner, P. Knowles, *J. Chem. Phys.* **82** (1985) 5053 (https://doi.org/10.1063/1.448627)
12. K. A. Peterson, T. B. Adler, H. J. Werner, *J. Chem. Phys.* **128** (2008) 084102 (https://doi.org/10.1063/1.2831537)
13. P. Knowles, C. Hampel, H. Werner, *J. Chem. Phys.* **99** (1993) 5219 (https://doi.org/10.1063/1.465990)
14. D. E. Woon, T. H. Dunning, *J. Chem. Phys.* **98** (1993) 1358 (https://doi.org/10.1063/1.464303)
15. A. Berning, M. Schweizer, H. Werner, P. J. Knowles, P. Palmieri, *Mol. Phys.* **98** (2000) 1823 (https://doi.org/10.1080/00268970009483386)
16. R. Renner, *Z. Phys.* **92** (1934) 172 (https://doi.org/10.1007/BF01350054)
17. M. Perić, S. D. Peyerimhoff, R. J. Buenker, *Mol. Phys.* **55** (1985) 1129 (https://doi.org/10.1080/00268978500101941)

18. M. Perić, S. D. Peyerimhoff, *J. Chem. Phys.* **102** (1995) 3685 (https://doi.org/10.1063/1.468599)
19. M. Perić, S. Jerosimić, R. Ranković, M. Krmar, J. Radić-Perić, *Chem. Phys.* **330** (2006) 60 (https://doi.org/10.1016/j.chemphys.2006.07.035)
20. M. Perić, *Chem. Phys.* **330** (2006) 73 (https://doi.org/10.1016/j.chemphys.2006.07.036)
21. M. Perić, H. Thümmel, C. M. Marian, S. D. Peyerimhoff, *J. Chem. Phys.* **102** (1995) 7142 (https://doi.org/10.1063/1.469108)
22. M. Perić, B. Ostojić, B. Engels, *J. Chem. Phys.* **105** (1996) 8569 (https://doi.org/10.1063/1.472641)
23. M. Perić, B. Ostojić, J. Radić-Perić, *Phys. Rep.* **290** (1997) 283 (https://doi.org/10.1016/S0370-1573(97)00018-5)
24. M. Perić, B. Ostojić, B. Schäfer, B. Engels, *Chem. Phys.* **225** (1997) 63 (https://doi.org/10.1016/S0301-0104(97)00225-5)
25. M. Perić, S. D. Peyerimhoff, *J. Mol. Spectrosc.* **212** (2002) 142 (https://doi.org/10.1006/jmsp.2002.8533)
26. M. Perić, S. D. Peyerimhoff, *J. Mol. Spectrosc.* **212** (2002) 153 (https://doi.org/10.1006/jmsp.2002.8534)
27. M. Perić, S. D. Peyerimhoff, in *The Role of Degenerate States in Chemistry*, I. Prigogine, S. A. Rice, M. Baer, G. D. Billing, Eds., Wiley, New York, 2002, p. 583 (https://doi.org/10.1002/0471433462.ch11)
28. M. Perić, Lj. Stevanović, *Int. J. Quantum Chem.* **92** (2003) 276 (https://doi.org/10.1002/qua.10484)
29. M. Perić, S. Jerosimić, M. Mitić, M. Milovanović, R. Ranković, *J. Chem. Phys.* **142** (2015) 174306 (https://doi.org/10.1063/1.4919285)
30. M. Mitić, M. Milovanović, R. Ranković, S. Jerosimić, M. Perić, *Mol. Phys.* **116** (2018) 2671 (https://doi.org/10.1063/1.4919285)
31. M. Perić, M. Petković, S. Jerosimić, *Chem. Phys.* **343** (2008) 141 (https://doi.org/10.1016/j.chemphys.2007.07.028)
32. M. Perić, R. Ranković, S. Jerosimić, *Chem. Phys.* **344** (2008) 35 (https://doi.org/10.1016/j.chemphys.2007.11.010)
33. M. Mitić, M. Milovanović, R. Ranković, S. Jerosimić, M. Perić *J. Serb. Chem. Soc.* **83** (2018) 439 (https://doi.org/10.2298/JSC171129001M)
34. B. C. Lanczos, *J. Res. Natl. Bur. Stand.* **45** (1950) 255 (https://archive.org/details/jresv45n4p255)
35. R. A. L. Cullum, J. K. Willoughby, *Algorithms for Large Symmetric Eigenvalue Computations*, Vols. I and II, Birkhäuser, Boston, MA, 1984
36. D. A. Hostutler, S.-G. He, D. J. Clouthier, *J. Chem. Phys.* **121** (2004) 5801 (https://doi.org/10.1063/1.1786924).